RSC Advances

Development of high performance high voltage insulator for power transmission line from blends of polydimethylsiloxane/ethylene vinyl acetate containing nanosilica

Dipankar Ghosh, Subhendu Bhandari, Tapan Kumar Chaki, Dipak Khastgir*

Rubber Technology Centre, Indian Institute of Technology Kharagpur

Kharagpur-721302, West Bengal, India

* Corresponding author: Dipak Khastgir

E-mail ID: khasdi@rtc.iitkgp.ernet.in

Phone: +91 - 3222 – 283192

Abstract

Ceramic materials are commonly used as outdoor insulator for high voltage power transmission line. Presently these ceramic insulators are replaced by composite polymeric insulators with silicone rubber (PDMS) housing, especially in industrial area with pollution. Silicone rubber is chosen for housing material because of their excellent aging resistance, electrical property, tracking resistance, stable hydrophobicity which in turn controls the tracking resistance. However, the material has seen deficiencies like poor mechanical strength and high cost. To improve mechanical properties and reduce cost, silicone rubber is blended with ethylene vinyl acetate copolymer (EVA). The optimum blend composition is found to be PDMS/EVA 60/40 w/w. But in doing so there is some reduction in hydrophobicity is observed, thus adversely affecting the tracking resistance. To improve hydrophobicity, the addition of nanosilica in the level of 6 phr is found to be the optimum. Thus high performance outdoor insulator can be produced from PDMS-EVA blend containing 6 phr nanosilica. Different types of accelerated aging test were performed on insulator samples to simulate their aging behavior under different real life aging process.

Key words: High voltage; Insulator; Nanocomposite; Polymer blend; Aging; Hydrophobicity

1. Introduction

Electrical insulator is one of the most important elements in power transmission systems. Weakness/flaw in the insulator may cause system failure leading to interruption in power supply. Conventional ceramic insulators are nowadays getting replaced by polymeric composite insulators.[1, 2] Nonceramic composite insulators consist of two components, i.e., the core made of composite of fiberglass with polyester or epoxy,[3, 4] and the housing, made of insulating polymers like silicone rubber (PDMS),[5, 6] ethylene vinyl acetate copolymer (EVA),[7] ethylene propylene diene rubber (EPDM) etc.[8, 9] The main advantages of polymeric insulators over conventional ceramic insulators are lighter in weight, ease of transportation (unbreakable) and installation in the electrical transmission line.[10] Silicone elastomer (PDMS) is the most preferred material for outer housing of composite insulator because of its better hydrophobicity[11] and less tendency to cause electrical flashover due to low leakage current possibilities.[12] Since PDMS does not get much affected by contaminants due to migration of low molecular weight fragments from the bulk to the surface which make the surface hydrophobic and also encapsulates the contaminant and maintain the hydrophobic character of the surface to a great extent.[13-15] This migration process is a continuous one, as a result, the hydrophobicity of the surface is maintained to a level required for preventing surface tracking (surface electrical flashover).[16] The detrimental environment effects on insulator due to the exposure in open atmosphere include UV rays and heat from sun, rain and moisture from dews.[17-20] The loss of low molecular weight fraction of PDMS from the surface due to accelerated aging like treatment with boiling water, exposure to heat or UV, causes reduction in low molecular weight fraction of PDMS on the surface. This process of loss and regain of low molecular weight fraction due to migration from the bulk to surface to retain the surface characteristics is not a perpetual process and cannot continue

lifelong. With the increase in aging time, the migration of low molecular weight fraction from the bulk reduces and regain of surface hydrophobicity is adversely affected thereby causing surface failure due to electrical tracking.[21-23] The surface of outdoor insulator should be hydrophobic nature. So that discrete water droplets formed by rain and or dew on insulator surface should not coalesce to form continuous channel causing surface tracking under high voltage application. How the environmental conditions adversely affect the surface characteristics of polymeric high voltage insulator are schematically represented with a figure in graphical abstract.

Materials with contact angle against water greater than 90° are considered to be hydrophobic in nature, whereas materials having contact angle less than 90° are considered to be hydrophilic.[24] The copolymer EVA (28% VA content), having contact angle (~ 92°) exists more or less in the border line,[25] whereas PDMS is with contact angle (~ 113°) is considered to be very good hydrophobic material[26] and has better ability to reduce leakage current and consequently has less chance of electrical discharge at the insulator surface.[12, 27]

Commercially available cheaper EVA (28% VA) has much better mechanical properties than PDMS. The blending of EVA with PDMS is expected to improve mechanical properties[28] while retaining the insulating characteristics of PDMS to a great extent. In reality, the judicial blending of these two polymers will compensate individual's property- deficiencies and provide a cost effective material for high voltage insulator application. However, the properties of insulator housing material not only depend on the base polymer/polymer blends, but also on the type, amount, shape and size of filler incorporated in the matrix polymer.[6, 29]

4

Alumina trihydrate (ATH) is used as a primary filler in large quantity in the insulator and it contributes to better erosion and tracking resistance.[30, 31] Some literatures reveal, the use of hydrophobic nanosilica as a secondary filler in polymer matrix to improve hydrophobicity.[32-37]

In the present work, an effort has been made to develop high performance insulator housing compound by partial replacement of PDMS with EVA to improve mechanical properties and cost effectiveness. The optimization of blend composition has been done and deficiencies encountered in blend compare to neat PDMS based insulator composite have been compensated through addition of nanosilica. The loading of nanosilica has also been optimized in insulator composition. The optimized blend composite was exposed to different accelerated aging conditions to assess the service performance of these insulators.

2. Experimental

2.1 Materials

Base polymer: 1. Silicone rubber (MQ/PDMS) source Momentive, Japan (TSE260- 7U). 2. EVA (28% vinyl acetate content), source NOCIL, India, grade- PILINE 2806, MFI @ 100ºC= 6 gm/cc, specific gravity= 0.95 gm/cc. Hydrophobic nanosilica (Aerosil® 812 S) source Evonik Industries, is modified grade of Aerosil® 300, after treatment with hexamethyldisilazane (HMDS). Alumina trihydrate (Grade- 4200) source Niknam Chemicals (P) Limited, average particle size 5 μm. Silicone oil (silicone fluid 350, Wacker Chemie), Paraffinic oil source Priyanka Refineries Pvt. Ltd.

2.2 Sample preparation and identification

The preparation of different blends of silicone rubber and EVA was accomplished in Brabender Plasti-Corder, PLE-330 at the temperature 120°C with rotor speed of 60 rpm. To evaluate the

5

effect of addition of nanosilica on different properties, a series of test samples were prepared. Nanofiller concentration was varied but restricted up to the maximum level of 12 phr for the investigations. At the first stage of mixing, EVA was added in the mixer and allowed to melt for 2 min, followed by the addition of PDMS (silicone rubber) and the mixing was continued up to 4 minutes thereafter the addition of filler, plasticizer (silicone oil + paraffinic oil), and antioxidant were done. Another 4 minutes is allowed for proper mixing of all added ingredients and the final addition of curative was done and mixing continued for 1 more minute. Then the whole mass was taken out from the Brabender and passed through the open mixing mill for final sheeting. Different samples were sheeted out from the mill and subjected to curing for optimum cure time at 165ºC as evaluated from Monsanto Rheometer.

2.3 Different modes of aging

Cured samples of all compositions were subjected to different accelerated aging tests through exposing them to boiling water, high temperature (150ºC) and UV light by artificial accelerated aging. The aging process under boiling water and high temperature (dry heat in aging oven) were continued up to 7 days. However, UV aging was carried out maximum up to 2 hr. An UV chamber with high power UV light obtained from Western Quartz, USA (1800 watt quartz lamp, wave length 250-350 nm) was used (ACS 21-22, cabinet built by Advance Curing System, Bangalore, India). The distance between sample and UV source was kept fixed at 7 cm. All the samples were naturalized for 24 hrs after aging prior to making measurement of different properties for these.

2.4 Characterizations

Different mechanical properties were measured using Hansfield Universal testing machine (H10KS) as per the ASTM D 412-98. The volume and surface resistivities of different samples were measured using Agilent High Resistance Meter (4339B) coupled with Agilent Resistivity Cell (16008B). Dielectric properties (dielectric constant and dielectric loss) were measured using Novocontrol Alpha-A Analyzer, Novocontrol Technologies, Germany. The static contact angle was measured using CA Goniometer (Rame-Hart Instrument Co, 264 F4). The hardness was measured using durometer type A (Shore Instruments and MFG Co, INC, USA, CV-71200, CONVELOADER). Electrical tracking analysis was done using Siemens and Halske Aktiengesellschaft instrument, Germany. The surface morphologies of different samples were analyzed using FESEM, field emission scanning electron microscopy (SUPRA 40, ZEISS, Germany), AFM, atomic force microscope (tapping mode, Agilent Technologies, 5500) and TEM, transmission electron microscopy (SUPRA 40, Karl ZEISS, Germany).

3. Result and discussion

3.1 Optimization of PDMS/EVA blend composition

Stress-strain plots of different PDMS/EVA blends and optimized blend with different nonosilica loading is presented in Fig. 1a and 1b respectively. Fig. 1a exhibits the increase in tensile strength and elongation at break with the increase in the proportion of EVA in the blends. This can be attributed to the strain induced crystallization of EVA which is semicrystalline in nature and act as a stronger component in the blend. That is why PDMS rich blends are comparatively weaker whereas EVA rich blends are stronger with higher elongation at break. The blend composition containing 60 wt% of PDMS shows adequate strength of about 3.6 MPa with

elongation at break 275%, and is quite suitable for application in high voltage insulator. The surface resistivity is considered as one of the important characteristics of high voltage insulator. The surface resistivity increases with the increase in PDMS concentration in the blend (Fig. 2a). However, the decrease in surface resistivity is relatively less for blend composition diluted with EVA up to 40 wt%, beyond which a sharp fall in resistivity is observed. The resistivity of the PDMS rich blend is mainly governed by the resistivity of continuous matrix PDMS rather than the dispersed EVA phase.[38] Again, the increase of contact angles with the increase in PDMS concentration in the blend implies more hydrophobic nature of the insulation surface required for the non-wettability characteristics of insulation surface (Fig. 2b). A blend with higher EVA content exhibits reduction in contact angle due to the presence of polar vinyl acetate group. In real life the insulator is exposed to an open atmosphere, resulting in the reduction of surface hydrophobicity. This leads to easy formation of water stream or water line from isolated water droplets generated from dews. These water lines cause electrical discharge on insulator surface under high voltage. Thus the suitable material for high voltage insulator should have enough mechanical strength, high surface resistivity, good hydrophobicity along with attractive price.

3.2 Optimization of nanofiller concentration in optimized blend composition

3.2.1. Mechanical Properties

The addition of nanosilica in the optimized blend composition (60/40 of PDMS/EVA) containing 100 phr of ATH and exhibits the increase in modulus and yield stress as revealed from stress-strain plots (Fig. 1b). It is noteworthy that the addition of nanosilica increases the elongation at break as well as tensile the strength for loading up to 6 phr, thereafter some fall in these two properties is observed when loading was increased up to 12 phr, this is mainly because of the dispersion problem of nanosilica at higher loading.[39] Fine filler particles with nano-dimension

have very high surface area and consequently very high surface energy leading to the formation of strongly bonded aggregates, difficult to disperse during mixing. So, the 6 phr loading of nanosilica has been found to be the optimum level with respect to improvement of overall properties.

3.2.2. FESEM analysis

As mentioned, the insulator property improvement depends not only on nanofiller concentration but also on its dispersion in the matrix polymer; the morphological investigation reveals improper dispersion at higher loading (> 6 phr).

FESEM of optimized PDMS/EVA blend with different loading of nanosilica are presented in Fig. 3a- f. It can be seen that up to 6 phr nanosilica filled composites show relatively smooth surface morphology. However, for system with filler loading beyond 6 phr, the increased surface roughness is apparent from FESEM picture. This is mainly because of improper dispersion of nanosilica particles at high loading (> 6 phr) due to formation of strong aggregates. The matrix polymer contains silicon as an element in the backbone, the filler also contains silicon. The existence of nanosilica on composite surface can be confirmed by EDX analysis.

The variation of % atomic concentration of elemental silicon (Si) with respect to elemental carbon (C) as measured from EDX (Fig. 4) confirms the increase in silica concentration on the sample surface almost linearly with the increase in nanosilica concentration.

3.2.3. Electrical Properties

Dielectric constant (ε') and dielectric loss (ε'') have been found to increase (Fig. 5a-b) with the decrease of frequency for all compositions especially below 10 Hz which may be attributed to increase in interfacial and space charge polarization. Above 10 Hz, the change in ε' and ε'' against frequency for all samples are relatively less. Moreover, the effect of nanosilica loading

on dielectric properties becomes more and more prominent at the lower frequency end. At 0.01 Hz, unfilled sample PES0 exhibits ε' and ε'' values of 23.7 and 121 respectively which drastically decrease to 16 and 37.5 for 6 phr loading samples, PES6. This phenomenon may be explained in the light of increase in restriction on polymer chain movement due to the increase of nanofiller concentration, thereby restricting the polarization (restricted movement of bound charges) process.[40-43] Generally lower the value of dielectric constant and loss for an insulating material better will be its electrical performance for high voltage applications.

The surface resistivity increases from 8.5×10^{14} for unfilled blend (PES0) to 2.5×10^{15} ohm.cm for 6 phr filled blend (PES6). The surface resistivity of 12 phr filled sample (PES12) however reduces to 1.5×10^{15} ohm.cm which is comparable to that of 3 phr loaded sample PES3 (1.6×10^{15}) ohm.cm (Fig. 6a).

Considering both bulk and surface electrical properties, it may be concluded that nanosilica can be dispersed with better homogeneity up to 6 phr loading, beyond which filler particles get clustered and non-uniformly distributed as evident from FESEM analysis (Fig. 3 and S1). The surface resistivity increases with nanosilica loading up to 6 phr thereafter some decrease in the resistivity is observed for loading more than 6 phr.

3.2.4. Contact angle

Being a surface characteristic, contact angle (CA) analysis also exhibits similar trend for hydrophobicity change against composition as observed for the surface resistivity. The contact angle is found to increase from 106º for the insulator PES0 to 116º for PES6 but with further increase in nanosilica loading it slightly decreases to 113º for the sample PES12 (Fig. 6b). This is mainly due to improper dispersion of nanosilica beyond 6 phr as discussed earlier.

3.2.5. Electrical tracking

The tracking voltage increases with nanosilica loading, from 28 kV for unfilled blend (PES0) to 33 kV for blend with 6 phr loading (PES6) however, it reduces to 31 kV for the 12 phr nanosilica filled system (PES12) (Fig. 7). Similar observations was reported in the literature.[44] Thus, the nanosilica concentration in the insulator formulation is found to be optimized at 6 phr loading in terms of electrical tracking performance.

3.3 Change in properties of insulator subjected to different aging

3.3.1. Mechanical properties

High voltage polymeric insulators used in power transmission lines have to operate in an open atmosphere under different climatic conditions throughout the year. Some basic detrimental factors of open atmosphere which adversely affect performance and service life of these polymeric insulators are (1) high temperature (heat from sun), (2) moisture (from rain and dew), (3) corrosive pollutants (from industrial gas, acid rain), (4) UV rays (from sunlight and corona discharge). All these environmental factors may operate simultaneously and have detrimental effects on the service life of an insulator. Different accelerated aging tests were performed to simulate the adverse effect of environmental conditions. The samples were subjected to the boiling water, dry heat (high temperature) as well as UV radiation.

From the stress-strain plots (Fig. 8a) of different aged samples along with fresh sample, it has been found that generally the modulus and tensile strength increase and elongation at break (EB) decreases for aged sample subjected to different aging condition except aging under UV rays. The samples subjected to heat aging for 7 days show appreciable increase in modulus and tensile strength (TS) but with severe loss in % elongation at break (EB). This may be attributable to the polymer chain scission along with high degree of crosslinking taking place during heat aging.

11

The insulator samples subjected to boiling water for 7 days also exhibit increase in TS and modulus and decrease in EB compared to the control (unaged) sample. But the decrease in EB in this case is somewhat less than that of the heat aged sample. However, UV radiation has the strongest detrimental effect on polymeric insulator. The UV aged sample exhibits both loss in TS and EB.

 The polymer aging has effect on its hardness. In fact hardness of a material is nothing but a very low strain modulus. For aging under boiling water, hardness increases from 80 Shore A (unaged) to 82 Shore A (aged), whereas for heat aging it increases up to 85 Shore A (aged) (Fig. 8b). Generally for polymer chain scission hardness should decrease whereas for inter-chain crosslinking it increases. For insulator samples subjected to dry heat aging and aging under boiling water the polymer crosslinking process predominates and consequently hardness shows net increase. On the other hand, for aging under UV radiation, chain scission predominates over crosslinking so a little reduction in hardness is observed, when sample shows 79 Shore A (UV aged) hardness which is marginally less compared to the unaged sample.   The probable mechanism of crosslinking and degradation of PDMS and EVA under UV radiation in presence of oxygen are shown in Fig. 9.

For ultraviolet (UV) radiation the photon energy is sufficient to cause on ionization, it means that, this radiation is capable of breaking chemical bonds. However compared to other ionization radiations like electron beam, X-ray, γ rays with higher frequencies, the photon energy associated with UV radiation is significantly less. So its effect on polymer is comparatively much less, and the process of polymer modification/degradation by UV rays is rather slow. However the photon energy associated with UV radiation is capable of breaking chemical bonds present in the polymer. In silicone rubber mainly three types of bonds exist and their breaking

energy is also in the following order, C-H ($\sim$ 337.2 kJ/mol) < C-C ($\sim$ 607 kJ/mol) < Si-O-Si ($\sim$ 798 kJ/mol). So the probability of breaking of C-H is the most and the breaking of this bond in PDMS leads to crosslinking process, whereas breaking of Si-O-Si leads to polymer degradation requiring the highest energy and this process will be the slowest one.[45]

However breaking of Si-O-Si bonds means the breakdown of backbone chains of the polymer which lead to reduction in tensile strength and elongation at break. The breakdown of C-H bonds lead to formation of crosslinks among polymer chains resulting in the increase in modulus and hardness as observed for some aged samples. In EVA the main chain consists of C-C linkages which have bond strength less than that of Si-O-Si bonds present in silicone elastomer (PDMS).

3.3.2. Electrical properties

Dielectric properties (dielectric constant ε' and dielectric loss/loss factor ε'') of high voltage insulator are important in power line AC- frequency range ($\sim$50-100 Hz). It is interesting to investigate the effect of different environmental condition on the change in dielectric properties of the insulator housing compound. The prolonged exposure of insulator in open atmosphere causes deterioration of insulating property of the samples. The change in dielectric constant with aging is marginal when insulator samples subjected to different types of aging (Fig. 10a). However, noticeable change in dielectric loss for samples subjected to different aging can be observed (Fig.10b). Dielectric loss signifies loss of electrical energy by the dielectric (insulator) when subjected to alternating (AC) electric field. Dielectric loss has different types of contribution from different types of polarization (restricted movement of bound charges). The most important contribution comes from dipolar and interfacial polarizations. Polarization again depends on concentration of bound charges per unit volume and their mobility. Dielectric loss is found to decrease with aging mainly because of restriction imposed on mobility of different type

of bound charges due to increase in crosslink density during heat aging and UV aging, whereas during aging under boiling water some increase in dielectric loss is observed mainly due to absorption of some moisture by the sample due to prolong exposure to water. Water is highly polar material. The increase in dielectric constant and loss factor of the insulator has negative effect on insulator performance, leading to increase in the chance of partial discharge under high voltage in micro-voids or defects generated in the insulator body due to different types of aging. The changes in surface resistivity for different types of aged samples have been shown in Fig. 10c. While for sample aged under boiling water, the surface resistivity decreases to 2.3×10^{15} ohm.cm from 2.5×10^{15} ohm.cm (fresh sample) whereas due to heat aging, the surface resistivity decreases drastically to 1.3×10^{15} ohm.cm and for UV aging to 1.1×10^{15} ohm.cm. The reduction in surface resistivity and hydrophobicity due to aging under different conditions has significant technical importance regarding performances of polymeric insulator under high voltage condition. In high voltage application that is under high potential difference, electrical discharge (electrical tracking) can take place on the insulator surface. This electrical tracking depends on surface resistivity which again depends on different extrinsic factors like deposition of pollutant, moisture or water droplets on the insulator surface, facilitating formation of low resistance path for electrical discharge. So long the water droplets formed on the insulator surface remains isolated the tracking is difficult to take place. If these droplets coalesce and form a bigger or continuous water line, electrical tracking can easily take place (dry band arching). In PDMS based insulators, low molecular weight (LMW) fragments of polymer, can migrates to the surface and can keep the surface hydrophobic in nature thereby preventing the formation of continuous water line necessary for tracking. With aging the concentration of LMW decreases in the matrix as well as their migration to surface. The possibility of surface tracking becomes more

14

probable with aging. This decrease in LMW fraction with aging is more due to UV aging compared to other type of aging as reflected from degree of reduction in contact angle.[46]

3.3.3. Change in hydrophobicity due to aging

The change of hydrophobicity of samples subjected to different types of aging are shown Fig. 11 and the actual pictures of the spreading of water droplets on the surface of aged samples have also been shown in Fig. 12. The hydrophobicity of different aged samples measured in terms of contact angle reduces due to aging (Fig. 11). Compared to contact angle for unaged sample (116º), it reduces to 113º for aging under boiling water, to 110º for dry heat aging and to108º for UV aging . The most significant reduction is observed for UV aging.

The detrimental effects mentioned earlier convert the hydrophobic surfaces to hydrophilic ones through removal of LMW fraction of PDMS. The presence of EVA in the blend has also some negative effect on hydrophobicity because the phenomenon of migration of LMW fraction from the bulk to surface as it happens in the case of PDMS is absent for EVA. During different accelerated aging, the loss of LMW fragments makes the surface hydrophilic in nature.[46] However, the decrement of hydrophobicity is found to be more during heat and UV aging than aging under boiling water, due to higher loss of LMW fragments by these two accelerated aging.[17, 47-49]

The developed compound exhibited better tracking characteristics (higher tracking voltage) compared to commercially available PDMS based insulation compounds (Fig. S3).

3.3.4. FESEM Analysis

Any aging process starts from the exposed surface of the insulator and continues to the depth of matrix. The extent of surface deterioration is important consideration during aging. As the failure process by electrical arching of the housing material is a surface phenomenon, and it depends on

surface condition. In fact the surface morphology and surface contamination play an important role on surface tracking behavior.

When composite sample with 6 phr filler loading is subjected to different kinds of aging, some roughness generates on the surfaces of aged samples. It can be visualized when comparison is made between surfaces of a sample before and after aging. The increase in surface roughness is mainly because of the polymer degradation occurred on the exposed surface subjected to boiling water, heat and UV radiation (Fig. 13a-c). In a neat sample, polymer chains thoroughly wet (coat) the filler particles and a smooth surface is observed for fresh sample. However after prolonged aging, the degraded polymer chains get easily removed leaving behind exposed filler particles which may be partially or wholly detached from bulk exhibiting surface roughness. The effect of aging on surface is more pronounced for UV aging (Fig. 13c), where surface has been found to be much more rough compared to surfaces of samples subjected to boiling water and heat. The surface degradation is found to be the least for aging under boiling water, whereas effect of heat aging is an intermediate. This indicates that during service, the UV radiation is the main detrimental factor for high voltage insulator working in an open atmosphere. This is further corroborated by AFM analysis done for unaged and different aged samples of the nanocomposite.

3.3.5. Atomic Force Microscopic Analysis

For samples under AFM analysis, the surface roughness are measured in terms of root mean square height (S_q), the maximum peak height (S_p), the maximum height (S_z) and arithmetic mean height (S_a) from 3D height images (Fig. 14a-d).[50, 51] Fig. S2 shows the 2D pictures of the 3D height images. These roughness parameters change with the types of aging, and found to be the highest for UV aged sample (Fig. 15 and Table S1). The S_q and S_a of the unaged sample are

found to be 32 and 26 nm respectively which increase to 58 and 44 nm for samples aged under boiling water aging and these values change to 87 and 67 nm for dry heat aging and 207 and 172 nm respectively for UV aging. The S_z of the unaged sample is 199 nm and it is increases to 390 nm for samples aged under boiling water but the values appreciably increases to 625 nm for heat aged samples and the maximum increase of 1120 nm is observed for UV aging. In fact magnitude of S_z for UV aged sample is more than 5 times larger than that of unaged sample.

With aging hydrophobic characteristic of insulator housing deteriorates, this is one of the most detrimental effects for the insulator when it works in the high voltage power transmission line. Also with aging, the surface roughness increases with time thereby introducing and increasing the site for mechanical failure (stress raiser). As a result mechanical properties for aged sample decrease with time as shown earlier. Under different aging conditions the size of these defects magnifies with time and the chance of accumulation of extraneous materials like moisture, pollutant, salts, carbon particles on insulator surface increases. All these external materials deposited on sample adversely affect surface electrical characteristic and thereby increase the probability of frequent electrical tracking on insulator surface ultimately leading to failure of both polymeric insulator housing and composite insulators. Defects and micro-void formation in the insulator housing also increases the chance of partial discharge under high voltage.

4. Summary and conclusions

PDMS/EVA 60/40 (w/w) blend has been found to be the most suitable polymer matrix which can replace 100% PDMS for making insulator housing. This blend is found to be better than neat PDMS with respect to mechanical properties and price. But the blend is inferior to neat PDMS with respect to hydrophobicity.

The decrease in hydrophobicity of PDMS due to blending with EVA can be compensated through incorporation of nanosilica as secondary filler in the composition. The addition of nanosilica is found to improve mechanical properties, hydrophobicity, surface resistivity and electrical tracking voltage. The optimum loading of secondary filler is found to be 6 phr, beyond which some properties deteriorate due to improper filler dispersion in the matrix polymer.

The losses in mechanical properties, electrical properties and surface hydrophobicity are observed for insulator samples subjected to different types of accelerated aging process. Of all aging tests, the exposure to high intensity UV radiation is found to cause the maximum overall reduction in properties. So it can be concluded that the atmospheric UV radiations from sunlight and corona discharge have the maximum detrimental effects on the polymeric insulator housing. The sever surface cracking is observed during UV aging through initial formation of micro-cracks on the surface which is responsible for deterioration of mechanical, electrical and hydrophobic characteristics of the insulator.

Acknowledgement

Notes and References

Electronic Supplementary Information (ESI) available: [TEM, AFM and Electrical tracking]

1.   M. R. Raghuveer, E. Kuffel, A. H. Qureshi and W. Opydo, *Power Apparatus and Systems, IEEE Transactions on*, 1978, **PAS-97**, 1672-1679.

2.   C. Aubin, C. Houdret, R. Mailfert and L. Pargamin, *Electrical Insulation, IEEE Transactions on*, 1981, **EI-16**, 290-296.

3.   H. Janssen, J. M. Seifert and H. C. Karner, *Dielectrics and Electrical Insulation, IEEE Transactions on*, 1999, **6**, 651-659.

4.   S. Kumara, I. R. Hoque, S. Alam, Y. V. Serdyuk and S. M. Gubanski, *Dielectrics and Electrical Insulation, IEEE Transactions on*, 2012, **19**, 1076-1083.

5.   P. Charalampidis, M. Albano, H. Griffiths, A. Haddad and R. T. Waters, *Dielectrics and Electrical Insulation, IEEE Transactions on*, 2014, **21**, 740-748.

6.   E. A. Cherney, *Dielectrics and Electrical Insulation, IEEE Transactions on*, 2005, **12**, 1108-1115.

7.   M. A. Pradeep, N. Vasudev, P. V. Reddy and D. Khastgir, *Journal of Applied Polymer Science*, 2007, **104**, 3505-3516.

8.   A. E. Vlastos and E. Sherif, *Power Delivery, IEEE Transactions on*, 1990, **5**, 406-414.

9.   G. Heger, H. J. Vermeulen, J. P. Holtzhausen and W. L. Vosloo, *Dielectrics and Electrical Insulation, IEEE Transactions on*, 2010, **17**, 513-520.

10.   J. Mackevich and M. Shah, *Electrical Insulation Magazine, IEEE*, 1997, **13**, 5-12.

11.   A. E. Vlastos and S. M. Gubanski, *Power Delivery, IEEE Transactions on*, 1991, **6**, 888-900.

12.   T. Sorqvist and S. M. Gubanski, *Dielectrics and Electrical Insulation, IEEE Transactions on*, 1999, **6**, 744-753.

13.   H. Homma, T. Kuroyagi, K. Izumi, C. L. Mirley, J. Ronzello and S. A. Boggs, *Dielectrics and Electrical Insulation, IEEE Transactions on*, 1999, **6**, 370-375.

14. H. Liu, G. A. Cash, R. D. Sovar, G. A. George and D. Birtwhistle, *Dielectrics and Electrical Insulation, IEEE Transactions on*, 2006, **13**, 877-884.

15. J. G. Wankowicz, S. M. Gubanski and W. D. Lampe, *Dielectrics and Electrical Insulation, IEEE Transactions on*, 1994, **1**, 604-614.

16. S. Kumagai and N. Yoshimura, *Dielectrics and Electrical Insulation, IEEE Transactions on*, 2001, **8**, 673-678.

17. Y. Bok-Hee and H. Chan-Su, *Dielectrics and Electrical Insulation, IEEE Transactions on*, 2005, **12**, 1015-1024.

18. B. Venkatesulu and M. J. Thomas, *Dielectrics and Electrical Insulation, IEEE Transactions on*, 2011, **18**, 418-424.

19. G. Bo, T. Youping, Z. Yiyang, L. Ruihai, Z. Fuzeng, X. Zhuo and L. Dong, 2013.

20. J. Jin, S. Chen and J. Zhang, *Polymer Degradation and Stability*, 2010, **95**, 725-732.

21. J. P. Reynders, I. R. Jandrell and S. M. Reynders, *Dielectrics and Electrical Insulation, IEEE Transactions on*, 1999, **6**, 620-631.

22. R. S. Gorur, G. G. Karady, A. Jagota, M. Shah and A. M. Yates, *Power Delivery, IEEE Transactions on*, 1992, **7**, 525-538.

23. G. Camino, S. M. Lomakin and M. Lazzari, *Polymer*, 2001, **42**, 2395-2402.

24. R. Forch, H. Schonheer and A. T. A. Jenkins, *Surface Design: Applications in Bioscience and Nanotechnology*, Wiley-VCH, Germany, 2009, 471.

25. I. O. Ucar, M. D. Doganci, C. E. Cansoy, H. Y. Erbil, I. Avramova and S. Suzer, *Applied Surface Science*, 2011, **257**, 9587-9594.

26. A. Mata, A. Fleischman and S. Roy, *Biomed Microdevices*, 2005, **7**, 281-293.

27.   R. S. Gorur, S. Sundhara Rajan and O. G. Amburgey, *Electrical Insulation, IEEE Transactions on*, 1989, **24**, 713-716.

28.   M. Ehsani, H. Borsi, E. Gockenbach, G. R. Bakhsahnde, J. Morshedian and N. Abedi, 2004.

29.   S. Ansorge, F. Schmuck and K. O. Papailiou, *Dielectrics and Electrical Insulation, IEEE Transactions on*, 2012, **19**, 209-217.

30.   J. V. Vas, B. Venkatesulu and M. J. Thomas, *Dielectrics and Electrical Insulation, IEEE Transactions on*, 2012, **19**, 91-98.

31.   S. Kumagai and N. Yoshimura, *Dielectrics and Electrical Insulation, IEEE Transactions on*, 2001, **8**, 203-211.

32.   H. Zhou, H. Wang, H. Niu, A. Gestos, X. Wang and T. Lin, *Advanced Materials*, 2012, **24**, 2409-2412.

33.   N. Garcia, E. Benito, P. Tiemblo, M. M. B. Hasan, A. Synytska and M. Stamm, *Soft Matter*, 2010, **6**, 4768-4776.

34.   X. Tang, T. Wang, F. Yu, X. Zhang, Q. Zhu, L. Pang, G. Zhang and M. Pei, *RSC Advances*, 2013, **3**, 25670-25673.

35.   A. Milionis, R. Ruffilli and I. S. Bayer, *RSC Advances*, 2014, **4**, 34395-34404.

36.   A. H. El-Hag, L. C. Simon, S. H. Jayaram and E. A. Cherney, *Dielectrics and Electrical Insulation, IEEE Transactions on*, 2006, **13**, 122-128.

37.   E. J. Park, J. K. Sim, M.-G. Jeong, H. O. Seo and Y. D. Kim, *RSC Advances*, 2013, **3**, 12571-12576.

38.   H. Amrollahi and M. Borhani, *International Journal of Engineering Research*, 2015, **4**, 69-72.

39.   J.-J. Park, *Transactions on Electrical and Electronic Materials*, 2012, **13**, 301-304.

40.   S. Hui, T. K. Chaki and S. Chattopadhyay, *Polymer Engineering & Science*, 2010, **50**, 730-738.

41.   S. Ju, M. Chen, H. Zhang and Z. Zhang, *eXPRESS Polymer Letters*, 2014, **8**, 682–691.

42.   A. Das, K. W. Stöckelhuber, R. Jurk, M. Saphiannikova, J. Fritzsche, H. Lorenz, M. Klüppel and G. Heinrich, *Polymer*, 2008, **49**, 5276-5283.

43.   R. A. Khare, A. R. Bhattacharyya, A. R. Kulkarni, M. Saroop and A. Biswas, *Journal of Polymer Science Part B: Polymer Physics*, 2008, **46**, 2286-2295.

44.   Y. Liu, Z. Li and B. Du, *Applied Physics Letters*, 2014, **105**, 102905.

45.   J. A. Dean, *Lange's Handbook of Chemistry*, McGraw-Hill, Inc., New York, 1999, 329-341.

46.   Y. Hirano, T. Inohara, M. Toyoda, H. Murase and M. Kosakada, *Dielectrics and Electrical Insulation, IEEE Transactions on*, 2001, **8**, 97-103.

47.   M. Ali and R. Hackam, *Dielectrics and Electrical Insulation, IEEE Transactions on*, 2009, **16**, 842-852.

48.   M. Ali and R. Hackam, *Dielectrics and Electrical Insulation, IEEE Transactions on*, 2008, **15**, 1368-1378.

49.   H. Hillborg and U. W. Gedde, *Dielectrics and Electrical Insulation, IEEE Transactions on*, 1999, **6**, 703-717.

50.   G. Momen, M. Farzaneh and R. Jafari, *Applied Surface Science*, 2011, **257**, 6489-6493.

51.   P. K. Maji and A. K. Bhowmick, *Journal of Applied Polymer Science*, 2013, **127**, 4492-4504.

Table 1. Designation of nanosilica filled PDMS/EVA nanocomposites.

Sample designation	Sample composition					
	P DMS (phr)	EVA (phr)	ATH (phr)	Silicone oil (phr)	Paraffinic oil (phr)	Nanosilica (phr)
PES0	60	40	100	10	5	0
PES3	60	40	100	10	5	3 (0.74 vol %)
PES6	60	40	100	10	5	6 (1.48 vol %)
PES9	60	40	100	10	5	9 (2.20 vol %)
PES12	60	40	100	10	5	12 (2.92 vol %)
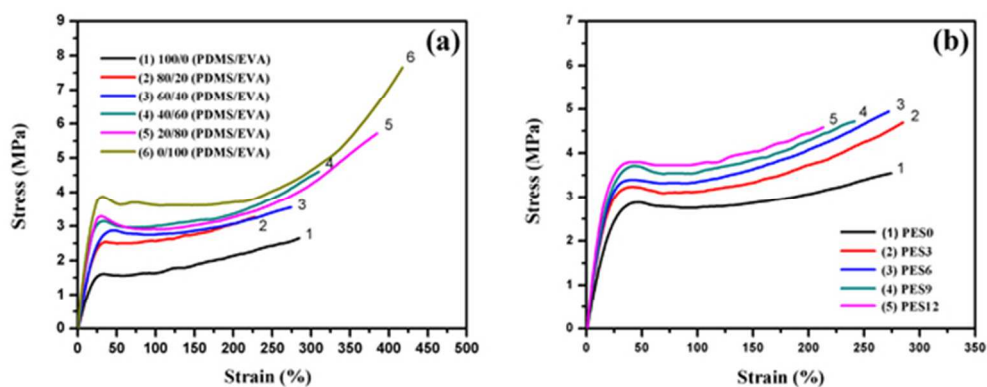
Fig. 1. Stress-strain plot of (a) PDMS/EVA blends with different PDMS: EVA ratio, (b) PDMS/EVA composites
with different concentration of nanosilica.
51x20mm (300 x 300 DPI)
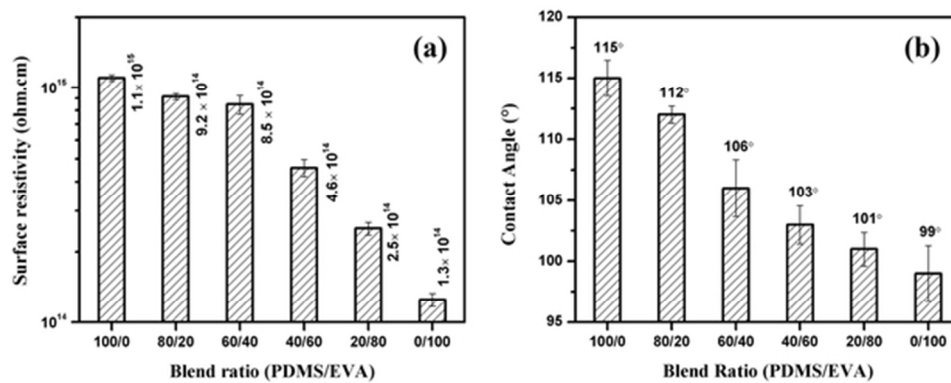
Fig. 2. Change in (a) surface resistivity and (b) contact angle of PDMS/EVA blends with different PDMS: EVA ratio.
54x23mm (300 x 300 DPI)
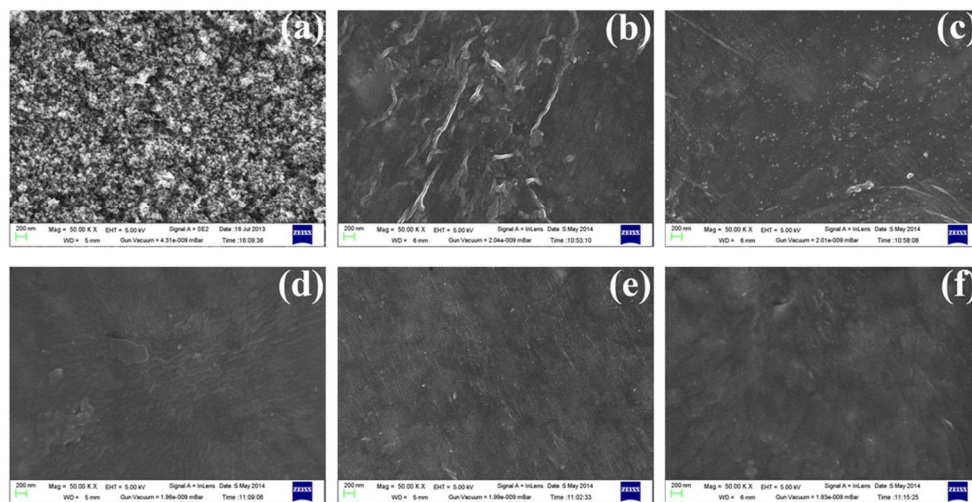
Fig. 3. FESEM micrograph of (a) nanosilica, (b) 0, (c) 3, (d) 6, (e) 9 and (f) 12 phr nanosilica filled nanocomposites.
91x47mm (300 x 300 DPI)
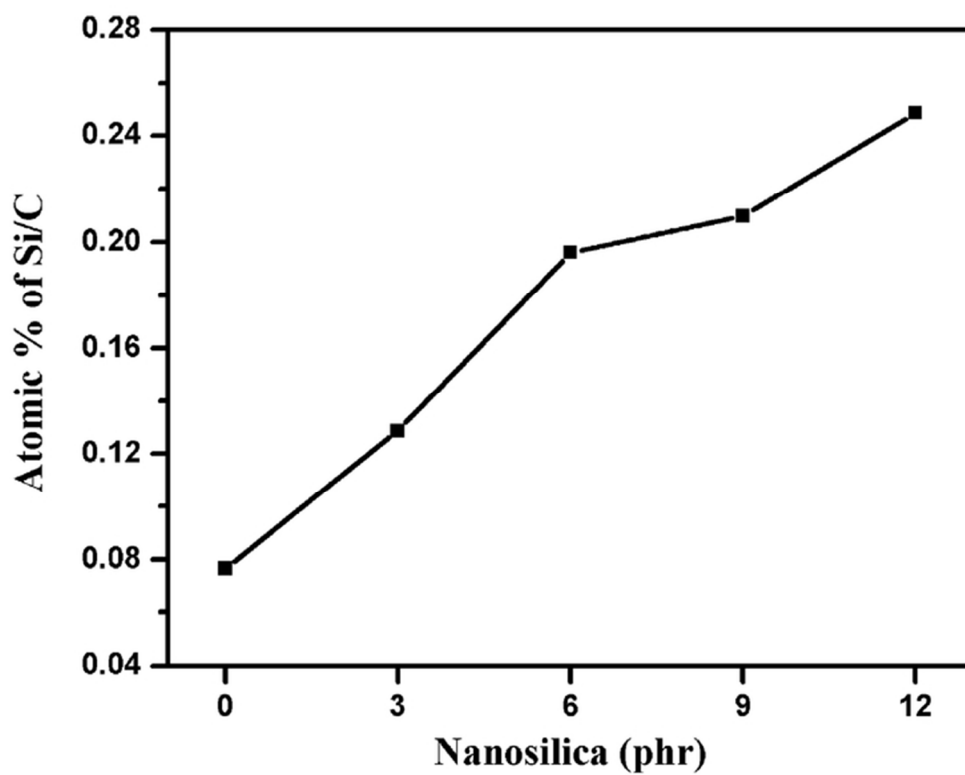
Fig. 4. Atomic % of Si:C with the increasing of nanofiller concentration.
63x50mm (300 x 300 DPI)
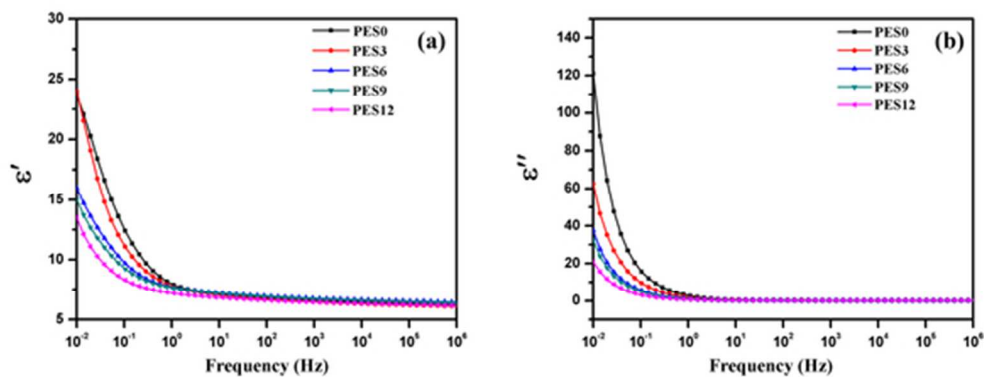
Fig. 5. Variation of (a) dielectric constant (ε') and (b) dielectric loss (ε'') against to applied frequency with various nanosilica content.
50x19mm (300 x 300 DPI)
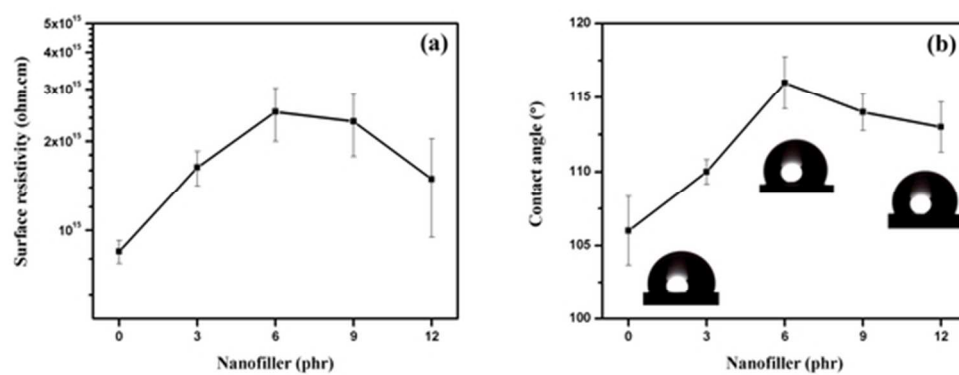
Fig. 6. Change of (a) surface resistivity and (b) contact angle with the variation of nanosilica concentration.
50x19mm (300 x 300 DPI)
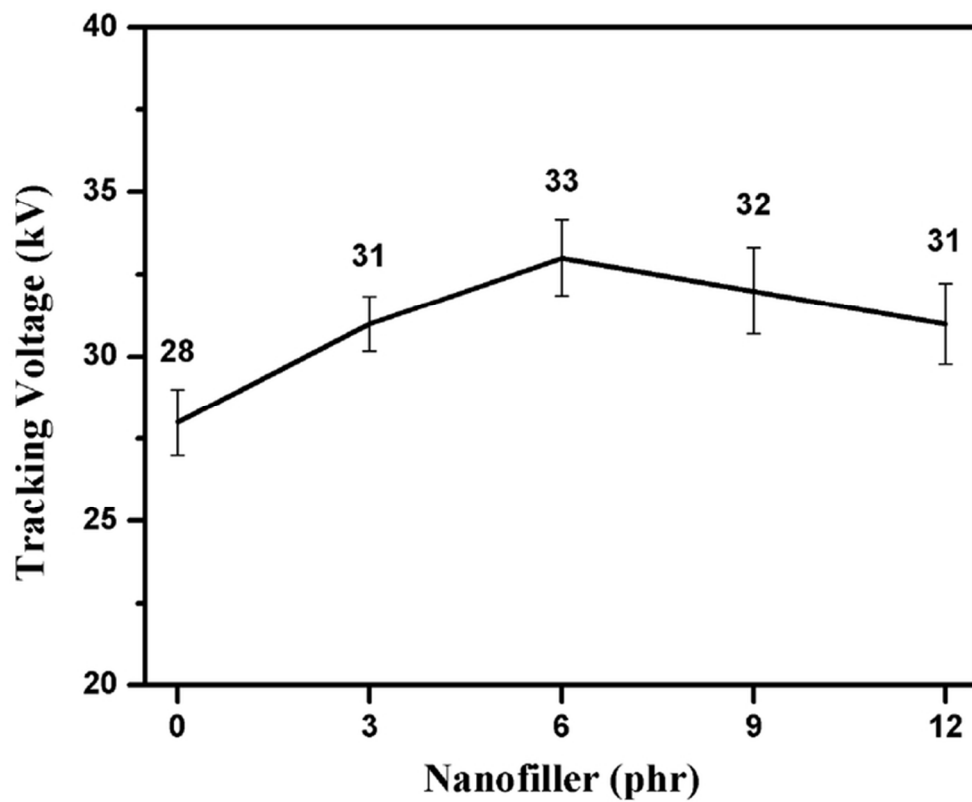
Fig. 7. Change of electrical tracking voltages with the variation of nanosilica concentration. 64x52mm (300 x 300 DPI)
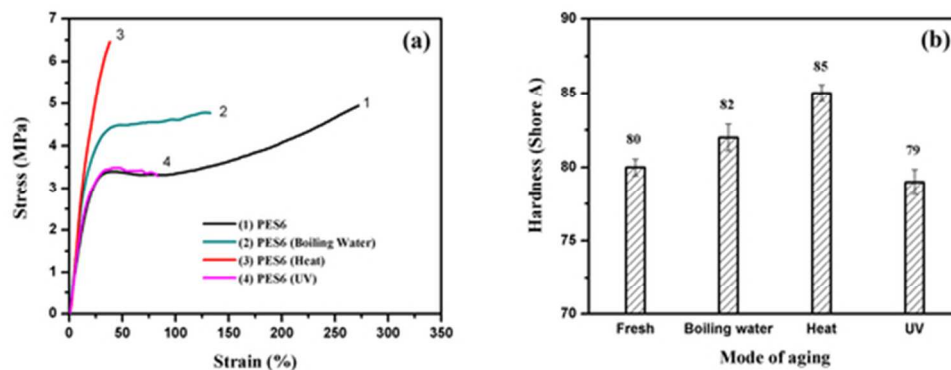
Fig. 8. (a) Stress-strain curve and (b) hardness of 6 phr nanosilica filled nanocomposite subjected to different type of aging.
49x18mm (300 x 300 DPI)
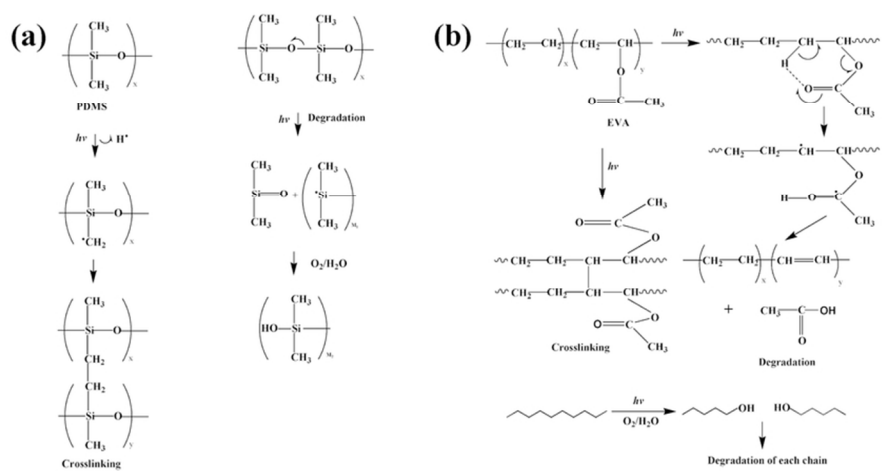
Fig. 9. Schematic illustration of the mechanism of crosslinking and degradation of (a) PDMS and (b) EVA under UV radiation.
80x37mm (300 x 300 DPI)
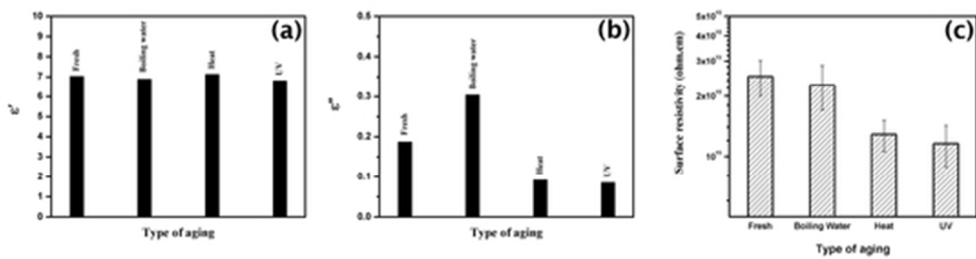
Fig. 10. Variation of (a) dielectric constant (ε') at 50 Hz, (b) dielectric loss (ε'') at 50 Hz and (c) surface resistivity under different kind of accelerated aging.
46x12mm (300 x 300 DPI)
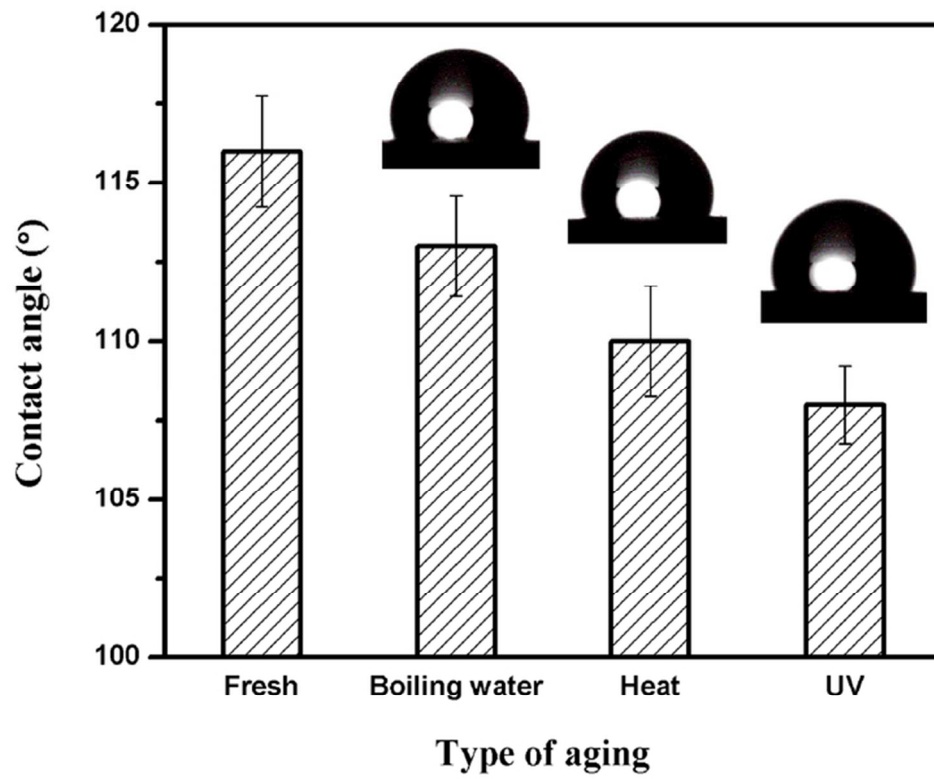
Fig. 11. Change in contact angle of unaged and different type of aged samples.
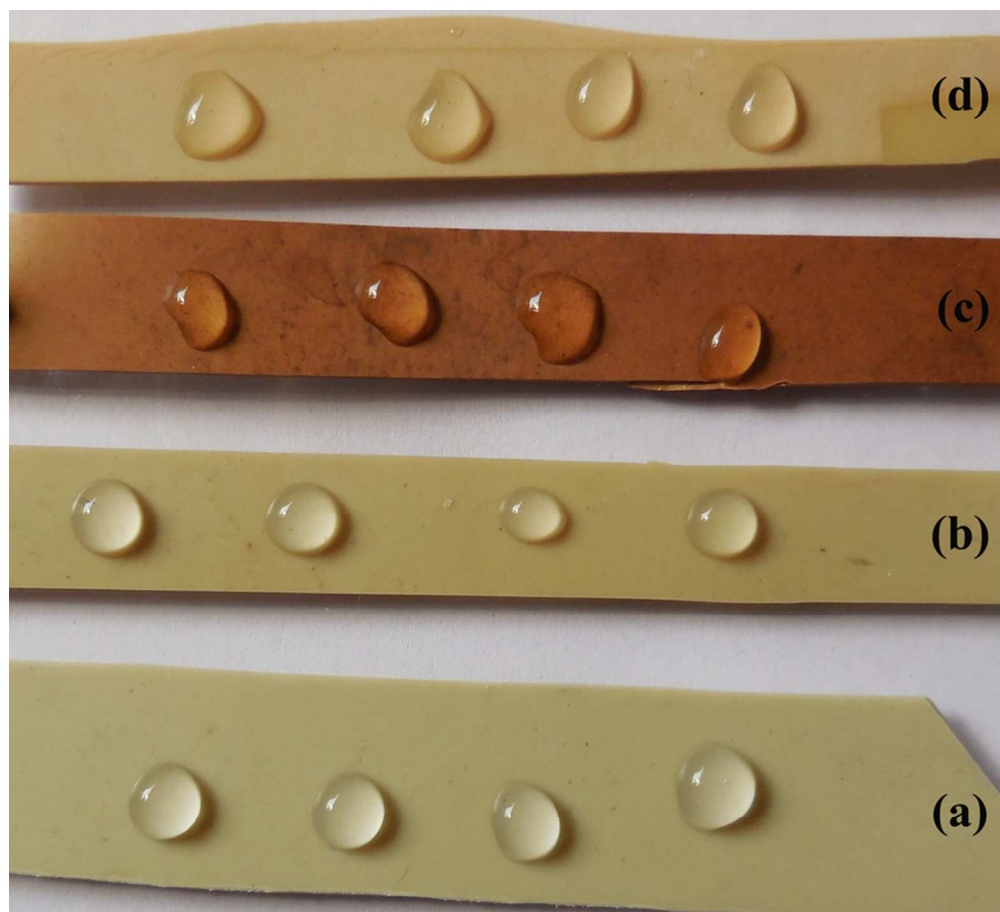65x53mm (300 x 300 DPI)

Fig. 12. Picture of spreading of water droplets on the different insulator surfaces (a) fresh sample, (b) boiling water aged sample, (c) heat aged sample and (d) UV aged sample.
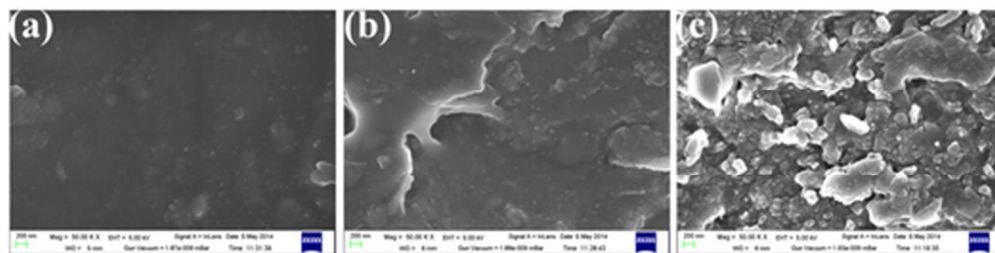72x65mm (300 x 300 DPI)

Fig. 13. FESEM micrograph of 6 phr nanosilica filled nanocomposites, under (a) boiling water, (b) heat and (c) UV aged.
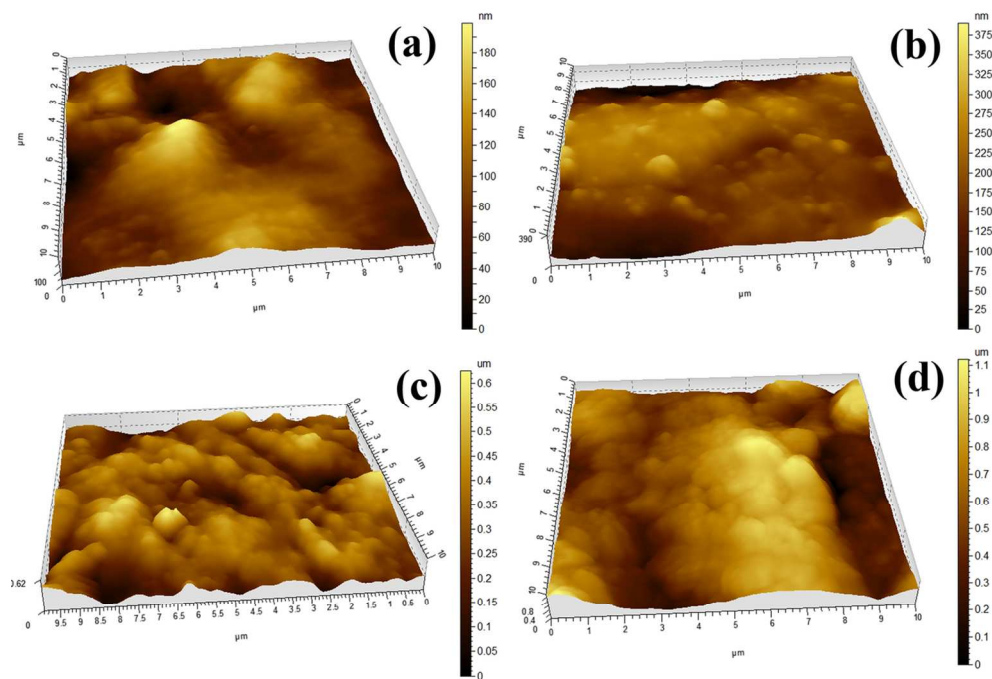44x11mm (300 x 300 DPI)

Fig 14. AFM 3D images of 6 phr nanosilica filled (a) unaged, (b) boiling water, (c) heat and (d) UV aged samples.
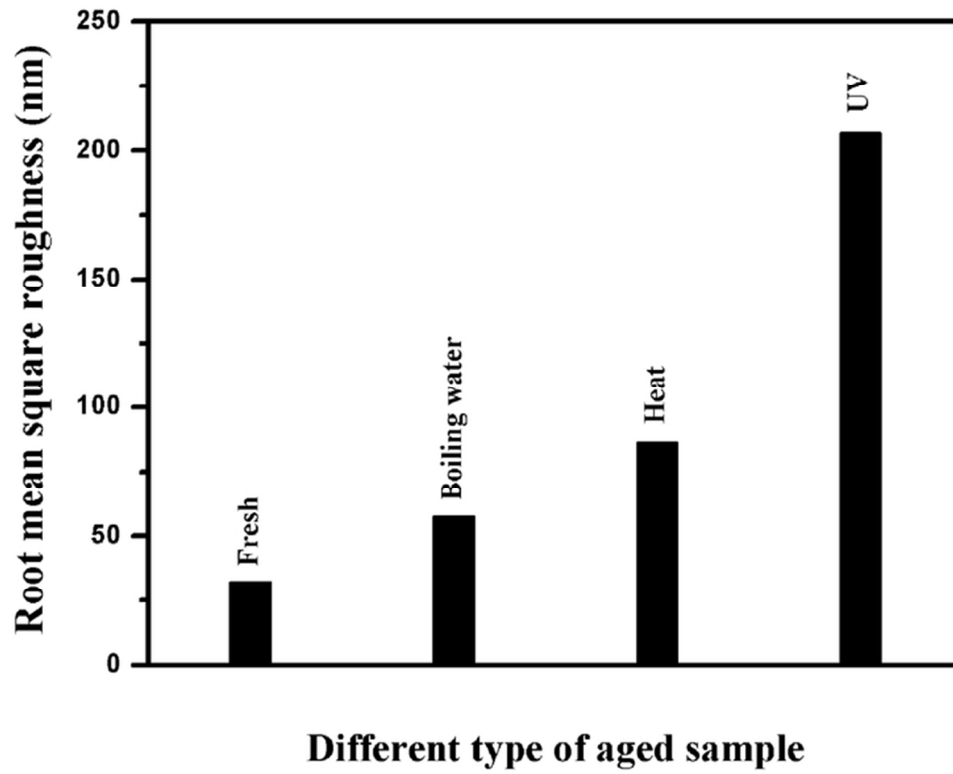121x85mm (300 x 300 DPI)

Fig. 15. Comparison root mean square height (Sq, nm) of 6 phr nanosilica filled unaged and aged samples. 64x51mm (300 x 300 DPI)